Research Article   Open Access

Transcriptomic Profiling of the Immune Response to Crowding Stress in Juvenile Turbot (*Scophthalmus maximus*)

Huanhuan Huo, Xiaoqiang Gao, Fan Fei, Fei Qin, Bin Huang and Baoliang Liu[*]

Key Laboratory of Sustainable Development of Marine Fisheries, Qingdao Key Laboratory for Marine Fish Breeding and Biotechnology, Yellow Sea Fisheries Research Institute, Chinese Academy of Fishery Sciences, Ministry of Agriculture, Qingdao 266071, China

[*]**Corresponding author:** Baoliang Liu, Yellow Sea Fisheries Research Institute, Chinese Academy of Fishery Sciences, Qingdao, 266071, China, Tel: +86 13969815257; E-mail: Liubl@ysfri.ac.cn

Abstract

In this study, juvenile turbot *Scophthalmus maximus* were vaccinated with attenuated Edwardsiella tarda and reared in two different densities, low density (LD, 5.25 ± 0.02 kg/m^2) as control groups and high density (HD, 20.53 ± 0.05 kg/m^2) as experimental groups, and only density as variable was considered. Five weeks after vaccination, the transcriptomes of spleen and head kidney from the turbot in the two density groups were analyzed with RNA-Seq technology. A total of 447 million reads were assembled into 41,136 genes with an average length of 1274 bp and N50 size of 2295 bp. A comparison of gene expression between HD and LD revealed 1155 differentially expressed genes (DEGs), including 246 significantly upregulated unigenes (fold-change>2) and 909 significantly downregulated unigenes (fold-change>2). Enrichment and pathway analysis of the immune-related DEGs showed the centrality of the Toll-like receptor signaling pathway, cytosolic DNA-sensing pathway and platelet activation in the host immune responses. The overexpressed inflammatory cytokines and downregulated signal-regulated cytokines are involved in these pathways. We inferred that overexpressed inflammatory cytokines indicate that cells suffer damage and downregulated signal pathway-related cytokines indicate the immune response is restrained in turbot under crowding stress. Our results increase understanding of the effect of crowding stress on immunosuppression and provide valuable information on healthful aquaculture strategies in juvenile turbot.

Introduction

Overcrowding as a chronic stressor in teleosts may increase the incidence of physical injuries [1-3] and susceptibility to diseases [4,5] and many suppress the immune response [6,7]. Many studies have demonstrated the influence of high stock density on the immune system [8]. Lymphocytopenia is a classic hematological response to stress and the number of lymphocytes can be decreased under chronic stress via the suppression of lymphocyte proliferation activities and the induction of apoptosis by B cells [9,10]. The stock density level has a direct relationship with the decrease in lymphocytes [11,12]. In addition, overcrowding can inhibit the production of specific antibodies IgM in fish blood by elevating cortisol levels [13]. The negative effect of high stock density on immunoglobulin M (IgM) production was observed when the sub-Antarctic notothenioid fish (*Eleginops maclovinus*) was challenged with *Piscirickettsia salmonis* protein extract [13]. Similarly, elevated cortisol levels inhibited IgM production in *Plecoglossus altivelis* when kept at a high stock density [14]. By increasing the production of relative oxygen species, a high stock density can also affect the level of oxidative stress and alter cellular functions [15]. However, our knowledge of how crowding stress suppresses the immune response is still limited.

The second-generation sequencing-based whole transcriptome analysis tool RNA-Seq allows the simultaneous and comprehensive characterization of all gene activities in a specific biological process. Accordingly, RNA-Seq has been employed to understand the immune events during a wider perspective on different biological settings in teleost fish [16,17]. RNA-Seq allows us not only to identify the gene and characterize the gene expression levels at the same time but also to elucidate host bacterial interactions [18]. To date, many immune studies in turbot have been performed using RNA-Seq following infection [19-21]. Using this sequencing technique, a large number of immune-related genes in several fish species were identified, including Japanese seabass (*Lateolabrax japonicus*), turbot (*S. maximus*), mud Loach (*Misgurnus anguillicaudatus*) and large yellow croaker (*Larimichthys crocea*) [22-25]. However, to our knowledge, no research has systematically characterized the immune strategies in turbot following attenuated *Edwardsiella tarda* vaccination and crowding stress at the transcriptomic level.

In this study, we aimed to determine the effects of crowding stress on the immune response in vaccinated fish. The juvenile turbot vaccinated with attenuated *E. tarda* were cultured at two different densities, high density (HD, 20.53 ± 0.05 kg/m^2) as experimental groups and low density (LD, 5.25 ± 0.02 kg/m^2) as control groups. After 5 weeks, the transcriptomes of the spleen and head kidney of vaccinated turbot from the two different density groups were analyzed. This transcriptomic study has enabled us to gain a better understanding of the effects of crowding stress on the immune response and identify a large number of differentially expressed target genes that bring us closer to the development of strategies designed to effectively combat pathogens. The identification of immune-relevant genes that could be potential markers for disease resistance is a means to establish a successful genetic breeding program. An understanding of the immune-related pathways in defense mechanisms is a relevant factor for enhancing the resistance of cultured fish to diseases.

Materials and Methods

Fish and experimental conditions

Healthy juvenile turbot weighing 150 ± 10 g were obtained from the farm of Shandong Oriental Ocean Sci-Tech Co. Ltd (Shandong, China), where the study was conducted. The fish were acclimated to the experimental environment for 15 days using a flow-through system. After vaccination with attenuated *E. tarda*, all of the fish were randomly assigned to two different stock densities: LD with 100 fish per tank (5.25 ± 0.02 kg/m^2) and HD with 400 fish per tank (20.53 ± 0.05 kg/m^2). Each density was tested with three replicates.

The fish were fed twice daily with commercial turbot feed (Ningbo Tech-Bank Co. Ltd, Zhejiang, China) and the daily ration was 1% of their body weight. During the test period, the water temperature was maintained at 16 ± 0.5°C with salinity at 28.2 ± 3%, dissolved oxygen at 8.0 ± 0.5 mg/l, and pH at 7.5 ± 0.3. The photoperiod was 12-h light and 12-h dark. No mortality was recorded during the experiment.

Sampling

In our previous study, the special antibody IgM in blood in vaccinated turbot approached maximum at the 5th week [26]. Therefore, 15 fish (5 fish per tank) were randomly collected after 5 weeks from each density group immediately after anesthetization with 0.05% tricaine methane sulfonate (MS-222, Sigma, St. Louis, MO, USA). The HD fish weighed 26.02 ± 0.05 kg/m^2 and the LD weighed 5.35 ± 0.02 kg/m^2 at sampling. The spleen and head kidney from 15 fish were dissected and pooled (five fish per pool). Samples were flash-frozen in liquid nitrogen and stored at −80°C prior to RNA extraction.

RNA extraction, library construction, and sequencing

Total RNA was extracted from the tissues using TRIzol Reagent (Invitrogen, Carlsbad, CA, USA) following the manufacturer's instructions. RNA degradation was monitored on 1% agarose gels. RNA concentration and purity were checked using a Nano-Drop 2000 spectrophotometer (Thermo, NewYork, MA, USA). Further, RNA integrity was assessed with the Agilent 2100 RNA 6000 Nano kit (Agilent Technologies, Santa Clara, CA, USA). High-quality samples (RNA integrity number>7.0, RNA concentration>100 ng/μl) were selected for high-throughput sequencing. For each sample, equal amounts of RNA from the three replicates were pooled for RNA-Seq library construction.

After total RNA was extracted, mRNA was enriched by oligo (dT) beads. The purified mRNA was fragmented into short fragments using fragmentation buffer and then used as a template for first-strand cDNA synthesis using random hexamers and reverse transcriptase. The second-strand cDNA was synthesized using DNA polymerase I and RNase H. Then the cDNA fragments were purified with a QiaQuick PCR extraction kit, end-repaired, poly(A) was added, and then ligated to Illumina sequencing adapters. The ligation products were size selected with agarose gel electrophoresis and amplified by PCR. Then the cDNA library was constructed from the cDNA synthesized using NEBNext UltraTM RNA Library Prep Kit for Illumina (New England Biolabs [NEB], Ipswich, MA, USA). The cDNA libraries were sequenced using Illumina HiSeqTM4000 by Gene Denovo Biotechnology Co. (Guangzhou, China).

De novo assembly of sequencing reads

To obtain high-quality clean reads for the transcript assembly, raw reads were filtered according to the following rules: removing reads containing more than 10% unknown nucleotides; removing low-quality reads containing more than 50% of low quality bases; removing reads containing adapters. The resulting high-quality sequences were de novo assembled into contigs and transcripts with Trinity software (http://trinityrnaseq.sf.net) [27]. To reduce data redundancy, transcripts with a minimum length of 200 bp were assembled and mapped to the reference transcriptome using the Bowtie2 short reads alignment tool under default parameters [28].

Gene annotation

All assembled unigenes were used as queries in searching the NCBI non-redundant (Nr) protein database and SwissProt protein database using the BLASTX program. The cutoff E-value was set at 1e−5 and only the top gene ID and name were initially assigned to each unigene. The unigenes were functionally annotated by gene ontology (GO) analysis with Blast2GO software (E-value<10−5). Kyoto Encyclopedia of Genes and Genomes (KEGG) pathway analysis was performed using KEGG Automatic Annotation Server (KASS) with default parameters [29].

Identification of differentially expressed genes

All clean sequencing reads from each of the cDNA libraries were mapped back to the transcriptome assembly using the software Bowtie2 with default settings. The reads aligned to each unigene in the alignment file were counted for each sample. These read counts were normalized as RPKM (reads per kilobase of transcripts per million fragments mapped) values [30] and further analysis to identify differentially expressed genes (DEGs) among the two different groups was conducted using a web tool DESeq. The false discovery rate (FDR) method was introduced to determine the threshold p-value in multiple tests to judge the significance of the difference in gene expression. If the FDR was <0.05 and there was at least a 2-fold difference in RPKM values among samples, the unigene was considered a significant DEG [31].

Experimental validation using qPCR

Twelve DEGs (Table 1) were selected randomly for validation of RNA-Seq data by qPCR using a SYBR Premix Ex Taq kit (Invitrogen) according to the manufacturer's instructions. The same RNA samples were used for both Illumina library synthesis and the qPCR verification assay. The first strand cDNA was obtained from 2 μg of total RNA using a PrimeScript 1st strand cDNA synthesis kit (Takara, Dalian, China). Melting curve analyses were performed following amplification. The specific primers used for qPCR are listed in Additional Table 1, and β-actin was used as an endogenous control. The thermal profile for SYBR Green qPCR was 95°C for 5 min, followed by 40 cycles of 95°C for 15 s, 60°C for 30 s. The relative gene expression was analyzed using the comparative threshold cycle method established by Livak et al. [32].

Ethical standards

All experiments were performed according to the Regulations on Animal Experimentation at Yellow Sea Fisheries Research Institute,

Qingdao, China. Following the experiment, all surviving fish were kept in laboratory.

Unigenes name		Primers sequence 5' to 3'	Number of base
CCL19	Forward	GCAGAACAGGGAACCGACA	19
	Reverse	CATCTACAGAATCCACCACACCA	23
CISH	Forward	GCGTGTGAGGTGCTGTAAGG	20
	Reverse	GACCAGAGAAGAAAGCAGACGAG	23
CXCL10	Forward	TGTTTGGCTGGTGTATGACTGG	22
	Reverse	GCTCTCTGCTTGTTCTCTGTGCT	23
CXCL13	Forward	GCATCACTGCCATCTTGACC	20
	Reverse	CAGTAGAGACGCAGACCATCACA	23
IL1R2	Forward	AGCAGCGGCAGAATGGTT	18
	Reverse	ACGCAGGTGAAGGTGGATTT	20
IL1β	Forward	CGTCGGAGCAAGACAACAAG	20
	Reverse	TGGGTCGTCTTTGAGGAGGT	20
IL18	Forward	CCTGATTCTCTACACAACCCAAAA	24
	Reverse	GAGATAAGTGTGAATACGGGGAATG	25
PIK3R	Forward	CAGGAAAGGAGGGAACAACAAG	22
	Reverse	AAGGAATCGTGGCGGTAGTG	20
SOCS3	Forward	CAGCTCGGACAACAGACACC	20
	Reverse	CGCAGTCAAAGTGGGGAAC	19
CCL20	Forward	TTCATCCTCAGCCTCGTCAT	20
	Reverse	CTGGAATGTGGAAGACAATGG	21
IFNA	Forward	CGTCAACATCTCCTTCCCAG	20
	Reverse	TACACTACCCATAATGCCCG	20
EPOR	Forward	ATCCACAATCGCAGCCTTC	19
	Reverse	GCTTCACACGGACTCGCAC	19
β-actin	Forward	TGAACCCCAAAGCCAACAGG	20
	Reverse	AGAGGCATACAGGGACAGCAC	21

Table 1: Primers used for qPCR validation of RNA-Seq.

Results

De novo assembly and annotation

To obtain the turbot transcriptome expression profile after vaccination, four cDNA libraries were constructed using spleen and head kidney from the two groups of HD and LD turbot. The results of transcriptome have been submitted to NCBI (SRA accession no. SRP129900). A total of 447 million clean reads were obtained for subsequent analysis after eliminating low-quality sequence and adaptor sequences from the original data sequence by quality analysis. The clean reads showed a high quality with a Q20 of 97.81% and Q30 of 94.83% (Table 2).

Groups	Sample	Clean Reads	Q20(%)	Q30(%)	GC Content(%)
High density	HS-1	5516370587	97.92	95.01	51.68
	HS-2	5516370587	98.06	95.31	51.55
	HS-3	5119739209	98.13	95.48	50.37
	HK-1	6155577277	98.15	95.51	50.91
	HK-2	5569206261	97.88	94.99	49.8
	HK-3	4518861022	98.07	95.35	50.74
Low density	LS-1	5411348450	98.03	95.26	51.82
	LS-2	5554985424	97.98	95.16	51.33
	LS-3	8186920388	97.99	95.19	51.5
	LK-1	5001629317	98.05	95.33	50.69
	LK-2	5272911727	97.96	95.12	50.88
	LK-3	5637638586	97.81	94.83	50.55

Table 2: The quality of clean reads. HS and HK represent the spleen and head kidney from high density respectively; LS and LK represent the spleen and head kidney from low density respectively.

According to the basic characteristics of transcripts, the distribution characteristics of the actual coverage of the reads are as follows: the nearer the 5'- and 3'- ends are, the lower the average sequencing depth is, but the overall homogenization degree is relatively high (Figure 1). Transcript de novo assembly was performed for the clean reads by Trinity. The total number and length of unigenes were 41,136 and 52,423,775 bp, respectively. The maximal length of the unigenes was 23,178 bp with an average length of 1274 bp (N50: 2295), the GC content was 49.13% (Table 3). These results indicate that the sequencing data was high-quality, and the unigenes could be used for subsequent annotation analysis.

Genes Num	GC percentage	N50	Max length	Min length	Average length	Total bases
41136	49.13%	2295	23178	201	1274	52423775

Table 3: Summary of de novo assembly of transcriptomic profiles of S. maximus.

To obtain comprehensive gene information, 41,136 unigenes were annotated by four databases including Nr, Clusters of orthologous groups for eukaryotic complete genomes (KOG), SwissProt and KEGG (Table 4). Annotation was matched successfully for 22,931 of the unigenes (22,806 in Nr, 20,101 in SwissProt, 16,035 in KOG, and 14,332 in KEGG) and 18,205 unigenes were without annotation. The distribution of 22,931 annotated unigenes from KEGG, KOG, Nr and SwissProt data are shown in Figure 2. In Nr annotation, 22,806 unigenes were matched to multiple species genomes, including Larimichthys crocea (31.58%), Stegastes partitus (25.76%), Oreochromis niloticus (5.68%), Notothenia coriiceps (5.16%), Cynoglossus semilaevis (4.92%), and others (26.88%) (Figure 3).
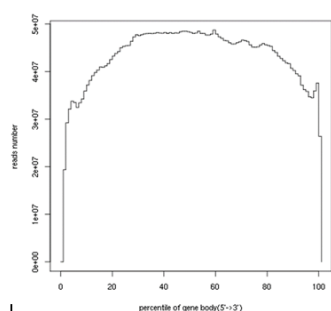
Figure 1: The homogeneity distribution of reads.

Total Unigenes	Nr	Swissprot	KOG	KEGG	Annotation genes	Without Annotation genes
41136	22806	20101	16035	14332	22931	18205

Table 4: The statistics of annotated unigenes of transcriptomic profiles in four databases.
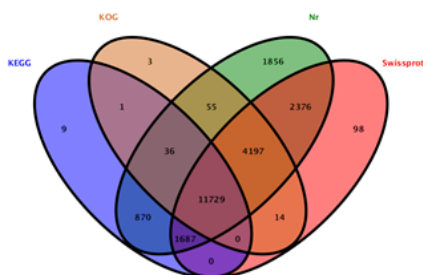

Figure 2: The venn of four database annotation. The distribution of a total 22931 annotated unigenes in KEGG, KOG, Nr and Swissprot database.
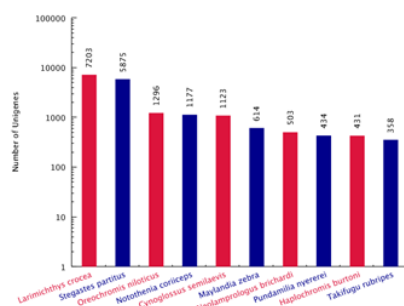

Figure 3: The top 10 species match to unigenes of S. maximus. The x-axis indicates the number of unigenes and the y-axis indicates matched species. From left to right, the matching degree from high to low.

Identification and analysis of DEGs

All of the unigenes were analyzed with DEG-Seq, whose threshold was restricted to q-value <0.005, |log2 (fold-change)|>1. A total of 1155 genes showed statistically significant differential expression in two immunologic organs that were compared in HD and LD turbot. In detail, 397 unigenes were identified as DEGs containing 146 significantly upregulated and 251 significantly downregulated unigenes in spleen. Additionally, 758 unigenes were identified as DEGs containing 100 significantly upregulated and 658 significantly downregulated unigenes in head kidney (Figure 4). In the statistical figures, we observed that the downregulation levels of DEGs were significantly higher than the upregulation levels after attenuated E. tarda administration. Among the 1155 DEGs, a group of 84 DEGs was shared between the two organs, 16 up- and 66 downregulated, and 2 either up- or downregulated depending on the organ.
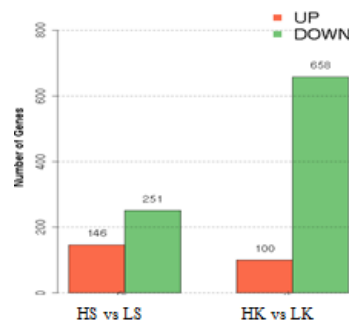

Figure 4: The statistics of different expression gene in spleen and head kidney. The red represents upregulated expressed genes and the green represents downregulated expressed genes.

## GO enrichment and pathway analysis

To further investigate the function of the DEGs, all were classified into three GO categories (biological process, molecular function, and cellular component) by Blast2GO. A total of 36 GO terms including 16 biological process terms, 12 cellular component terms and 8 molecular functions terms were associated with spleen DEGs (Figure 5). A total of 42 GO terms including 19 biological process terms, 13 cellular component terms, and 10 molecular functions terms were associated with head kidney DEGs (Figure 6). Analysis of level 2 GO term distribution showed that cellular process, binding, and cell were the most common annotation terms in the three GO categories. Among these, the immune system process was retained for further pathway analysis, although it was not the most significant.

A total of 401 unigenes were homologous to immune-relevant genes based on the KEGG annotation and were classified into 15 functional pathways (Table 5). Furthermore, through immune-related DEG screening, 10 DEGs (Table 6) were assigned to six immune-relevant pathways, including the RIG-I-like receptor signaling pathway, cytosolic DNA-sensing pathway, Toll-like receptor (TLR) signaling pathway, NOD-like receptor signaling pathway, chemokine signaling pathway, and platelet activation. Among these immune-relevant pathways, we focused on significantly changed signaling pathways (P<0.05) such as the TLR signaling pathway, cytosolic DNA-sensing pathway, and platelet activation.
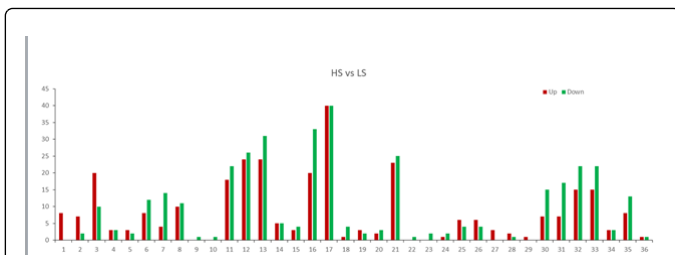
Figure 5: Gene ontology (GO) enrichment analysis of the differently expressed genes. A total of 36 GO terms including 16 biological process terms (1-16), 12 cellular component terms (17-28) and 8 molecular functions terms in spleen (29-36). Note: 1 Locomotion; 2 immune system process; 3 response to stimulus; 4 biological adhesion; 5 multi-organism process; 6 developmental process; 7 multicellular organismal process; 8 localization; 9 reproduction; 10 reproductive process; 11 biological regulation; 12 metabolic process; 13 single-organism process; 14 signaling; 15 cellular component organization or biogenesis; 16 cellular process; 17 binding; 18 molecular function regulator; 19 nucleic acid binding transcription factor activity; 20 transporter activity; 21 catalytic activity; 22 structural molecule activity; 23 signal transducer activity; 24 molecular transducer activity; 25 extracellular region part; 26 extracellular region; 27 extracellular matrix; 28 cell junction; 29 supramolecular fiber; 30 membrane part; 31 membrane; 32 cell; 33 cell part; 34 macromolecular complex; 35 organelle; 36 organelle part.

number of annotation genes represents expressed genes in the corresponding pathway in this study.
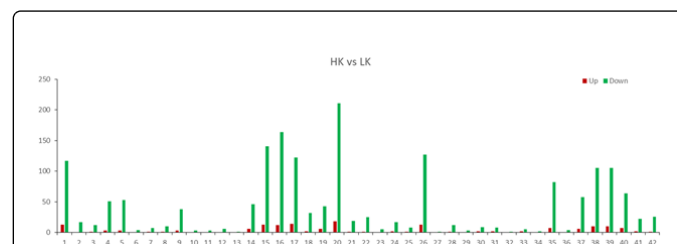
Figure 6: Gene ontology (GO) enrichment analysis of the differently expressed genes. A total of 42 GO terms including 19 biological process terms (1-19), 13 cellular component terms (20-32) and 10 molecular functions (33-42) terms in head kidney. Note: 1 biological regulation; 2 immune system process; 3 biological adhesion; 4 multicellular organismal process; 5 developmental process; 6 behavior; 7 growth; 8 locomotion; 9 cellular component organization or biogenesis; 10 reproduction; 11 reproductive process; 12 multi-organism process; 13 rhythmic process; 14 localization; 15 single-organism process; 16 cellular process; 17 metabolic process; 18 signaling; 19 response to stimulus; 20 binding; 21 nucleic acid binding transcription factor activity; 22 molecular transducer activity; 23 transcription factor activity, protein binding; 24 transporter activity; 25 molecular function regulator; 26 catalytic activity; 27 antioxidant activity; 28 signal transducer activity; 29 structural molecule activity; 30 extracellular region; 31 extracellular region part; 32 extracellular matrix component; 33 membrane-enclosed lumen; 34 extracellular matrix; 35 organelle; 36 cell junction; 37 membrane part; 38 cell; 39 cell part; 40 membrane; 41 organelle part; 42 macromolecular complex.

Immune related signaling pathway	KO identifier	DEGs	Annotation genes
Chemokine signaling pathway	Ko04062	2	8
Platelet activation	Ko04611	2	8
Toll-like receptor signaling pathway	Ko04620	7	124
NOD-like receptor signaling pathway	Ko04621	3	69
RIG-I-like receptor signaling pathway	Ko04622	3	84
Cytosolic DNA-sensing pathway	Ko04623	4	56
Antigen processing and presentation	Ko04612	-	3
Hematopoietic cell lineage	Ko04640	-	1
Natural killer cell mediated cytotoxicity	Ko04650	-	2
T cell receptor signaling pathway	Ko04660	-	1
B cell receptor signaling pathway	Ko04662	-	2
Fc epsilon RI signaling pathway	Ko04664	-	2
Fc gamma R-mediated phagocytosis	Ko04666	-	1
Leukocyte transendothelial migration	Ko04670	-	3
Intestinal immune network for IgA production	Ko04672	-	37

Table 5: KEGG pathway enrichment analyses of the immune related differently expressed genes and annotation genes. The symbol "-" represents the number of differently expressed genes were zero. The

Gene Name	Unigene ID	Head kindey	Spleen
ADCY1	Unigene0024880	-3.43596	-1.80757
TLN	Unigene0013036	-2.18731	-2.9128
MAPK1_3	Unigene0027102	-1.15902	-0.48954
PIK3R	Unigene0031916	-1.42467	-1.01278
DDX3X	Unigene0000801	-1.50048	-0.62096
CXCL10	Unigene0027837	0.857201	1.093359
CXCL9	Unigene0005965	0.508599	1.28799
IL1β	Unigene0036119	0.472608	1.494326
IFN-α	Unigene0038981	1.234147	2.647089
IL18	Unigene0004586	-0.70697	-1.28315

Table 6: The information of immune related DEGs. Bold values indicate significantly changed relative to the low density groups. The positive numbers indicate up-regulation and the negative numbers indicate down-regulation.

Validation of RNA-Seq profiles by qPCR

To validate the RNA-Seq data, 12 DEGs were selected randomly for qPCR. Although, the test unigenes displayed different expression levels

(Figure 7), in general, the qPCR results showed a positive correlation with RNA-Seq data, indicating the reliability and accuracy of the RNA-Seq expression analysis.
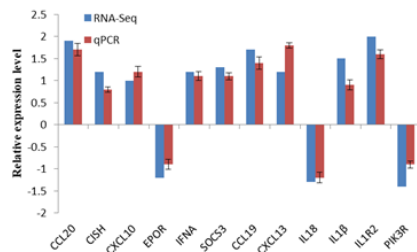
Figure 7: Validation of RNA-seq data by using qPCR. X-axis, pairwise comparison groups; Y-axis, fold change in gene expression. CCL20, CISH, IFNA, SOCS3, IL1R2 and PIK3R were detected in head kidney; CXCL10, EPOR, CCL19, CXCL13, IL18 and IL1β were detected in spleen. The qPCR data were given in mean ± SD, n=3.

Discussion

RNA-Seq technology uses RNA-Seq sequence data to provide a complete picture of the transcriptome under study (global annotation) and simultaneously provide quantitative data related to differential gene expression. In the present study, we have obtained the transcriptome comparative data of S. maximus spleen and head kidney under two different culture densities and have acquired 41,136 unigenes after assembling and filtration. RNA-Seq technology can annotate successfully in the absence of a genome dependent upon the other existent genome resources and expressed sequence tag collections [33]. Although the turbot genome was released and was available in the European Nucleotide Archive, the mapping percent was very low; therefore, we used the BLASTX program to annotate the unigenes in an approach adopted by other studies [20].

In Nr annotation, only 1123 unigenes were matched to Cynoglossus semilaevis (4.92%) genomes. The origin of flatfish has been the focus of long-term controversy [34]. Phylogenetic studies show low interfamily/suborder statistical support among flatfish, especially between the Psettoidei and Pleuronectoidei, and the low phylogenetic support is considered evidence of a polyphyletic origin [35]. Genetic evidence on the diversification of flatfish have been reported using genome sequencing of the turbot and the tongue sole [36,37], suggesting that different strategies are adapted for demersal life [34].

A total of 1155 DEGs were categorized into many categories based on GO annotation and pathway analyses. These categories included the immune system, which is the key category we focus on. Below we highlight three key constituents of the immune system, the TLR signaling pathway, the cytosolic DNA-sensing pathway, and platelet activation, which were all influenced significantly by crowding stress.

TLR signaling pathway

Recognition of pathogen-associated molecular patterns (PAMPs) is essential for the activation of innate immunity and it is carried out by TLRs. TLRs, specific families of pattern recognition receptors, are responsible for detecting microbial pathogens and generating innate immune responses. Pathogen recognition by TLRs provokes rapid

activation of innate immunity by inducing the production of pro-inflammatory cytokines and upregulation of costimulatory molecules as well as priming the adaptive immune system [38-40]. Efficient immune responses depend upon a close interaction between the innate and adaptive immune systems. TLRs serve as an important link between the innate and adaptive immune responses [41]. Importantly, TLRs participate in the direct regulation of the adaptive immune response, possibly as costimulatory molecules [42]. Dendritic cells stimulated directly or indirectly by TLRs from pathogens mature into a specific form and are able to activate a specific immune response that is appropriate for the elimination of the pathogen [43]. In diseases, TLRs also participate in inflammation and immune responses that are driven by self-, allo- or xeno-antigens [40].

In our study, inflammatory cytokines such as interleukin (IL)-1β and interferon (IFN)-ⵧ were markedly upregulated in spleen when turbot suffered crowding stress. It is well-known that the protective properties of these inflammatory factors remove the adverse stimulus in the first line of an organism's defense against pathogen invasion, but a stronger inflammatory response can lead to tissue damage as well [44]. IL-10 is also (anti) inflammatory cytokine, may decrease the production of pro-inflammatory cytokines and keep the immune system in balance. In our study, there was no significant upregulation of IL-10, indicating that the inflammatory cytokines were overexpressed. For similar reasons, markedly upregulated IL-10 inhibited IL-1β expression in Schizothorax prenanti after poly(I:C) challenge [44]. Chemokines have a broad spectrum of effects on innate immunity, such as becoming a promoter to adhere various types of leukocyte to inflammatory loci in early immunity [45,46]. Research has shown that turbot CXC chemokines were dramatically and rapidly induced at 5 h after challenge and the expression of CXC chemokine was not observed until after 12 h [42]. In our study, CXCL9 and CXCL10 were upregulated at the 5th week, which may indicate the overexpression of CXC chemokines. In addition, we found that PIK3R was markedly downregulated in spleen. PI3k inhibition leads to the suppression of IL-10 but induced IL-1β expression [47]. The PI3ks are lipid kinases that are activated by receptor tyrosine and suppress cell apoptosis and promote cell growth and play important roles in the immune response [48]. Downregulated PIK3R signifies that crowding stress is disadvantageous to the immune response.

In head kidney transcriptomic data, no inflammatory cytokines and costimulatory molecules were observed to be upregulated or downregulated. However, PIK3R and MAPK1-3 were dramatically downregulated in the TLR signaling pathway. The downregulation of MAPK1-3 indicates the suppression of extracellular signal-regulated kinases (ERK), which are widely expressed protein kinase intracellular signaling molecules involved in maintaining cell survival and mediating intracellular signal transduction in response to a variety of stimuli [49-51]. Some studies show that upregulated ERK plays a key role in environmental adaptation processes such as protecting cells from stress [52,53]. In our study, downregulated ERK signifies that crowding stress damages spleen cells.

Cytosolic DNA-sensing pathway

Specific families of pattern recognition receptors are responsible for detecting foreign DNA from invading microbes or host cells and generating innate immune responses. Cytosolic DNA sensors detect intracytoplasmic double-stranded DNA and signal through a central adaptor protein, stimulator of IFN genes (STING), which recruits and activates the downstream TBK1/IRF3 signaling axis to induce the

production of type IFN [54,55]. Type IFN are critical for innate immune defense against viral infections [56,57]. Furthermore, cytosolic DNA also activates STING-dependent and STING-independent autophagy to promote host defense against bacterial infection [58,59]. Studies by Rengaraj et al. have shown that the cytosolic DNA-sensing pathway is the most important immune pathway in necrotic enteritis-induced chickens [60]. Similar results were obtained in our study, the DEG enrichment in the cytosolic DNA-sensing pathway are significantly up regulated in spleen. IL-1β, IFN-α, and CXCL10 are up regulated, but IL-18 is down regulated in the cytosolic DNA-sensing pathway. Studies have confirmed that IL-18 is important for regulating the Th1 and Th2 immune response [61]. The down regulation of IL-18 will attenuate the ability of the spleen cell immune response. In head kidney, DEGs are not enriched in the cytosolic DNA-sensing pathway indicating that spleen and head kidney play different roles in the immune response.

Platelet activation

It has become obvious that platelets are not only cell fragments that plug the leak in a damaged blood vessel but also key components in the innate immune system, which is supported by the presence of TLRs on platelets [62]. Recently platelets have been reported to express TLR2, 4 and 9, reinforcing their role as primitive immune cells in host defense [63,64]. As platelets are usually the first cells to respond to a wound, they have an important role in the immune response to infection through their activation [65,66]. Platelets acting as components of the innate immune system detect the presence of infectious agents and coordinate the response to the pathogen [67]. When activated, platelets secrete over 300 proteins [68] including the bioactive molecules adenosine diphosphate (ADP) and serotonin to reduce blood loss, cytokines and chemokine recruiting leucocytes to deal with any potential infection, and antimicrobial peptides to kill pathogens. The activation of platelets leads to the secretion of antimicrobial peptides, although many bacteria have become resistant to these peptides [69].

In our study, AC and TLN were significantly downregulated in the platelet activation pathway in head kidney. TLN is a master regulator of platelet integrin activation in vivo. If there is a lack of TLN, the platelet aggregation function will be damaged severely and integrin αIIbβ3 activation will also be inhibited [70,71]. TLN downregulation decreases ligand binding to cellular integrins resulting in restrained platelet and leukocyte function. AC, the second messenger cyclic adenosine monophosphate (cAMP) and cAMP-dependent protein kinase A are important mediators in determining the response of a cell to external stimuli [72,73]. Activated AC increases the intracellular cAMP level, which enhances the host defense [74]. The downregulation of AC will attenuate the response of a cell to external stimuli by decreasing cAMP levels.

Apart from the nine genes mentioned above, one gene DDX3X is significantly downregulated in the RIG-I-like receptor signaling pathway. DDX3X participates in regulating mRNA translation and some signaling pathways [75,76]. DDX3X directly regulates Wnt/β-catenin signaling and INF-induced signal pathways [75,77]. DDX3X is responsible for detecting viral pathogens and generating innate immune responses. Vaccinia virus protein K7 can combine with DDX3X to suppress the innate immune response [78]. Downregulated DDX3X indicates that the innate immune response is inhibited.

Conclusion

Using RNA-Seq-based transcriptome profiling, we assessed, for the first time, the transcriptomic responses of turbot cultured in different densities following vaccination with attenuated E. tarda. A total of 1155 DEGs were annotated in four databases. We identified immune-related DEGs compared in high and low stock densities. After RNA-Seq data analysis and qPCR validation, we observed that immune-related DEGs were primarily enriched in the TLR signaling pathway and cytosolic DNA-sensing pathway in spleen, and platelet activation occurs in head kidney. The inflammatory cytokines, IL-1β, IFN-α, CXCL10, and CXCL9, and signal-regulated cytokines, PIk3R, MAPK1-3, AC, and TLN, are involved in these pathways. Overexpressed inflammatory cytokines and downregulated signal-regulated cytokines show that cells suffer damage and the immune response is restrained when turbot is stressed due to crowding. Although further functional studies are needed to characterize the key immune factors governing the turbot immune responses, these results can provide a foundation to evaluate the relationship between immunosuppression and crowding stress.

Acknowledgment

References

1. Juell, JE, Fosseidengen JE (2004) Use of artificial light to control swimming depth and fish density of atlantic salmon (salmo salar) in production cages. Aquaculture 233: 269-282.

2. Turnbull J, Bell A, Adams CE, Bron JE, Huntingford F (2005) Stocking density and welfare of cage farmed atlantic salmon: application of a multivariate analysis. Aquaculture 243: 121-132.

3. North BP, Turnbull JF, Ellis T, Porter MJ, Migaud H et al. (2006) The impact of stocking density on the welfare of rainbow trout (Oncorhynchus mykiss). Aquaculture 255: 466-479.

4. Ellis AE (2001) Innate host defense mechanisms of fish against viruses and bacteria. Dev Comp Immunol 25: 827-839.

5. Tort L (2011) Stress and immune modulation in fish. Dev Comp Immunol 35: 1366-1375.

6. Nardocci G, Navarro C, Cortés P, Imarai M, Montoya M, et al. (2014) Neuroendocrine mechanisms for immune system regulation during stress in fish. Fish Shellfish Immunol, 40: 531-538.

7. Yarahmadi P, Miandare HK, Hoseinifar SH, Gheysvandi N, Akbarzadeh A (2015) The effects of stocking density on hemato-immunological and serum biochemical parameters of rainbow trout (Oncorhynchus mykiss). Aquaculture International, 23: 55-63.

8. Jia R, Liu BL, Feng WR, Han C, Huang B, et al. (2016) Stress and immune responses in skin of turbot (Scophthalmus maximus) under different stocking densities. Fish Shellfish Immunol 55: 131-139.

9. Pulsford AL, Crampe M, Langston A, Glynn PJ (1995) Modulatory effects of disease, stress, copper, tbt and vitamin e on the immune system of flatfish. Fish Shellfish Immunol 5: 631-643.

10. Verburg-van Kemenade BL, Nowak B, Engelsma MY, Weyts FAA (1999) Differential effects of cortisol on apoptosis and proliferation of carp B-lymphocytes from head kidney, spleen and blood. Fish Shellfish Immunol 9: 405-415.

11. Cristea V, Mocanu M, Antache A, Docan A, Dediu L, et al. (2012) Effect of stocking density on leuckocyte reaction of Oncorhynchus mykiss (walbaum, 1792). Lucrari Stiintifice Zootehnie Si Biotehnologii 45: 31-36.

12. Zebral YD, Zafalon-Silva B, Mascarenhas MW, Robaldo RB (2015) Leucocyte profile and growth rates as indicators of crowding stress in pejerrey fingerlings (Odontesthes bonariensis). Aquaculture Research 46: 2270-2276.

13. Vargas-Chacoff L, Martínez D, Oyarzún R, Nualart D, Olavarría V, et al. (2014) Combined effects of high stocking density and Piscirickettsia salmonis treatment on the immune system, metabolism and osmoregulatory responses of the sub-antarctic nothothenioid fish Eleginops maclovinus. Fish Shellfish Immunol 40: 424-434.

14. Iguchi K, Ogawa K, Nagae M, Ito F (2003) The influence of rearing density on stress response and disease susceptibility of ayu (Plecoglossus altivelis). Aquaculture 220: 515-523.

15. Neiva B, Ronaldolima DL, Bernardo B, Dafre AL, Nuñer APO (2010) Growth, biochemical and physiological responses of Salminus brasiliensis with different stocking densities and handling. Aquaculture 301: 22-30.

16. Peatman E, Li C, Peterson BC, Straus DL, Farmer BD, et al. (2013) Basal polarization of the mucosal compartment in Flavobacterium columnare susceptible and resistant channel catfish (Ictalurus punctatus). Mol Immunol 56: 317-327.

17. Zhu J, Li C, Ao Q, Tan Y, Luo Y et al. (2015) Trancriptomic profiling revealed the signatures of acute immune response in tilapia (Oreochromis niloticus), following streptococcus iniae, challenge. Fish Shellfish Immunol 46: 346-353.

18. Chen SL, Liu Y, Dong XL, Meng L (2010) Cloning, characterization, and expression analysis of a CC chemokine gene from turbot (Scophthalmus maximus). Fish physiol Biochem 36: 147-155.

19. Robledo D, Ronza P, Harrison PW, Losada AP, Bermúdez R, et al. (2014) RNA-Seq analysis reveals significant transcriptome changes in turbot (Scophthalmus maximus) suffering severe enteromyxosis. BMC Genomics, 15: 1149.

20. Gao C, Fu Q, Su B, Zhou S, Liu F, et al. (2016) Transcriptomic profiling revealed the signatures of intestinal barrier alteration and pathogen entry in turbot (Scophthalmus maximus) following vibrio anguillarum, challenge. Dev Comp Immunol 65: 159-168.

21. Ronza P, Robledo D, Bermúdez R, Losada AP, Pardo BG, et al. (2016) RNA-Seq analysis of early enteromyxosis in turbot (Scophthalmus maximus): new insights into parasite invasion and immune evasion strategies. Int J Parasitol 46: 507-517.

22. Xiang LX, He D, Dong WR, Zhang YW, Shao JZ (2010) Deep sequencing-based transcriptome profiling analysis of bacteria-challenged Lateolabrax japonicus reveals insight into the immune-relevant genes in marine fish. Bmc Genomics, 11: 1-21.

23. Pereiro P, Balseiro P, Romero A, Dios S, Forn-Cuni G, et al. (2012) High-throughput sequence analysis of turbot (Scophthalmus maximus) transcriptome using 454-pyrosequencing for the discovery of antiviral immune genes. Plos One 7: e35369.

24. Long Y, Li Q, Zhou B, Song G, Li T, et al. (2013) De novo assembly of mud loach (Misgurnus anguillicaudatus) skin transcriptome to identify putative genes involved in immunity and epidermal mucus secretion. Plos One 8: e56998.

25. Yin F, Gao Q, Tang B, Sun P, Han K, et al. 2016. Transcriptome and analysis on the complement and coagulation cascades pathway of large yellow croaker (Larimichthys crocea) to ciliate ectoparasite cryptocaryon irritans infection. Fish Shellfish Immunol 50: 127-141.

26. Huo H, Yin S, Jia R, Huang B, Lei J, et al. (2017) Effect of crowding stress on the immune response in turbot (Scophthalmus maximus) vaccinated with attenuated edwardsiella tarda. Fish Shellfish Immunol 67: 353-358.

27. Grabherr MG, Haas BJ, Yassour, M, Levin JZ, Thompson DA, et al. (2011) Full-length transcriptome assembly from RNA-Seq data without a reference genome. Nat Biotechnol 29: 644-652.

28. Li R, Yu C, Li Y, Lam TW, Yiu SM, et al. (2009) SOAP2: an improved ultrafast tool for short read alignment. Bioinformatics 25: 1966-1967.

29. Zhang X, Wang S, Chen S, Chen Y, Liu Y, et al. (2015) Transcriptome analysis revealed changes of multiple genes involved in immunity in Cynoglossus semilaevis during vibrio anguillarum infection. Fish Shellfish Immunol 43: 209-218.

30. Mortazavi A, Williams BA, McCue K, Schaeffer L, Wold B, et al. 2008. Mapping and quantifying mammalian transcriptomes by RNA-Seq. Nat Methods 5: 621-628.

31. Li G, Zhao Y, Liu Z, Gao C, Yan F, et al. (2015) De novo assembly and characterization of the spleen transcriptome of common carp (Cyprinus carpio) using illumina paired-end sequencing. Fish Shellfish Immunol 44: 420-429.

32. Livak KJ, Schmittgen TD (2001) Analysis of relative gene expression data using real-time quantitative PCR and the 2(-Delta Delta C(T)) Method. Methods 25: 402-408.

33. Mackenzie S, Boltaña S, Novoa B (2012) 13-developments in genomics relevant to disease control in aquaculture. Infectious Disease Aquaculture p331-352.

34. Robledo D, Hermida M, Rubiolo JA, Fernández C, Blanco A, et al. (2016) Integrating genomic resources of flatfish (Pleuronectiformes) to boost aquaculture production. Comp Biochem Physiol Part D Genomics Proteomics, 21: 41-55.

35. Campbell MA, Chen WJ, López JA (2014) Molecular data do not provide unambiguous support for the monophyly of flatfishes (pleuronectiformes): a reply to Betancur-R and Ortí. Molecular Phylogenetics & Evolution 75: 149-153.

36. Chen S, Zhang G, Shao C (2014) Whole-genome sequence of a flatfish provides insights into ZW sex chromosome evolution and adaptation to a benthic lifestyle. Nat genetics 46: 253.

37. Antonio F, Diego R, André C (2016) Whole genome sequencing of turbot (Scophthalmus maximus; pleuronectiformes): a fish adapted to demersal life: DNA Research 23: 181-192.

38. Pasare C, Medzhitov R (2004) Toll-like receptors: linking innate and adaptive immunity. Microbes & Infection 6: 1382-1387.

39. Werling D, Jann OC, Offord V, Glass Ej, Coffey TJ (2009) Variation matters: tlr structure and species-specific pathogen recognition. Trends in Immunol 30: 124-130.

40. Liu G, Zhang L, Zhao Y (2010) Modulation of immune responses through direct activation of toll-like receptors to t cells. Clin Exp Immunol 160: 168-175.

41. de Souza AL, Seguro AC (2008) Two centuries of meningococcal infection: from vieusseux to the cellular and molecular basis of disease. J Med Microbiol 57: 1313-1321.

42. Liu Y, Chen SL, Meng L (2007) Cloning, characterization and expression analysis of a novel cxc chemokine from turbot (Scophthalmus maximus). Fish Shellfish Immunol 23: 711-720.

43. Dulay AT, Buhimschi CS, Zhao G (2009) Soluble tlr2 is present in human amniotic fluid and modulates the intraamniotic inflammatory response to infection. J Immunol 182: 7244-7253.

44. Du X, Li Y, Li D (2017) Transcriptome profiling of spleen provides insights into the antiviral mechanism in Schizothorax prenanti, after poly (i: c) challenge. Fish Shellfish Immunol 62: 13-23.

45. Bagasra O (1997) The immunobiology of interferon-gamma inducible protein 10 kd (ip-10): a novel, pleiotropic member of the c-x-c chemokine superfamily. Cytokine Growth Factor Reviews 8: 207-219.

46. Yoshie O, Imai T, Nomiyama H (2001) Chemokines in immunity. Adv Immunol 78: 57-110.

47. Marshall NA, Galvin KC, Corcoran AM (2012) Immunotherapy with pi3k inhibitor and toll-like receptor agonist induces ifn-γ+il-17+ polyfunctional t cells that mediate rejection of murine tumors. Cancer Res 72: 581-591.

48. Shi Z, Hodges VM, Dunlop EA (2010) Erythropoietin-induced activation of the JAK2/STAT5, PI3K/Akt, and Ras/ERK pathways promotes malignant cell behavior in a modified breast cancer cell line. Mol Cancer Res 8: 615-626.

49. Dou F, Yuan LD, Zhu JJ (2005) Heat shock protein 90 indirectly regulates erk activity by affecting raf protein metabolism. Acta Biochimica ET Biophysica Sinica 37: 501-505.

50. Ikeyama S, Kokkonen G, Shack S (2002) Loss in oxidative stress tolerance with aging linked to reduced extracellular signal-regulated kinase and akt kinase activities. Faseb Journal 16: 114-116.

51. Rehani K, Wang HC, Kinane D (2009) Toll-like receptor-mediated production of il-1ra is negatively regulated by gsk3 via the mapk erk1/2. J Immunol 182: 547-553.

52. Helmreich EJM (2001) Components of signaling networks: linkers and regulators. The biochem cell signal. Oxford University Press, New York.

53. Padmini E, Tharani J (2014) Fourier Transform Infrared Spectroscopic Study on HSP70 and ERK in Fish Hepatocytes during Pollution Induced Stress. Int J Res Chem Env 4: 114-125.

54. Wu J, Chen Z J (2014) Innate immune sensing and signaling of cytosolic nucleic acids. Annual Rev Immunol 32: 461.

55. Roers A, Hiller B, Hornung V (2016) Recognition of endogenous nucleic acids by the innate immune system. Immunity 44: 739-754.

56. Schneider WM, Chevillotte MD, Rice CM (2014) Interferon-stimulated genes: a complex web of host defenses. Annual Rev Immunol 32: 513-545.

57. Yang K, Wang J, Wu M (2015) Mesenchymal stem cells detect and defend against gammaherpesvirus infection via the cgas-sting pathway. Scientific Reports 5: 1-9.

58. Liang Q, Seo GJ, Choi YJ, et al. (2014) Crosstalk between the cgas dna sensor and beclin-1 autophagy protein shapes innate antimicrobial immune responses. Cell Host & Microbe 15: 228-238.

59. Watson R, Bell S, Macduff D, Kimmey J, Diner E, et al. (2015) The cytosolic sensor cgas detects Mycobacterium tuberculosis, dna to induce type i interferons and activate autophagy. Cell Host Microbe 17: 811.

60. Rengaraj D, Truong AD, Lee SH (2016) Expression analysis of cytosolic dna-sensing pathway genes in the intestinal mucosal layer of necrotic enteritis-induced chicken. Vet Immunol Immunopathol 170: 1-12.

61. Nakanishi K, Yoshimoto T, Tsutsui H (2001) Interleukin-18 is a unique cytokine that stimulates both th1 and th2 responses depending on its cytokine milieu. Cytokine Growth Factor Rev 12: 53-72.

62. Cox D, Kerrigan SW, Watson SP (2011) Platelets and the innate immune system: mechanisms of bacterial-induced platelet activation. J Thromb Haemost J 9: 1097.

63. Cognasse F, Hamzeh H, Chavarin P (2005) Evidence of Toll-like receptor molecules on human platelets. Immunol Cell Biol 83: 196-198.

64. Aslam R, Speck ER, Kim M (2006) Platelet Toll-like receptor expression modulates lipopolysaccharide-induced thrombocytopenia and tumor necrosis factor-α production in vivo. Blood 107: 637-641.

65. Fitzgerald JR, Foster TJ, Cox D (2006) The interaction of bacterial pathogens with platelets. Nat Rev Microbiol 4: 445-57.

66. Yeaman MR (2010) Bacterial-platelet interactions: virulence meets host defense. Future Microbiol 5: 471-506.

67. Garraud O, Cognasse F (2010) Platelet toll-like receptor expression: the link between "danger" ligands and inflammation. Inflamm Allergy Drug Targ 9: 322-333.

68. Coppinger JA, Cagney G, Toomey S (2004) Characterization of the proteins released from activated platelets leads to localization of novel platelet proteins in human atherosclerotic lesions. Blood 103: 2096-2104.

69. Yeaman MR, Bayer AS, Koo SP (1998) Platelet microbicidal proteins and neutrophil defensin disrupt the staphylococcus aureus cytoplasmic membrane by distinct mechanisms of action. J Clin Invest 101: 178-187.

70. Griffiths EK, Krawczyk C, Kong YY (2001) Positive regulation of t cell activation and integrin adhesion by the adapter fyb/slap. Science 293: 2260-2263.

71. Han J, Lim CJ, Watanabe N (2006) Reconstructing and deconstructing agonist-induced activation of integrin αiibβ3. Curr Biol 16: 1796-1806.

72. Grandoch M, Roscioni SS, Schmidt M (2010) The role of epac proteins, novel camp mediators, in the regulation of immune, lung and neuronal function. Br J Pharmacol 159: 265-284.

73. Bhattacharjee R, Xiang W, Wang Y (2012) cAMP prevents TNF-induced apoptosis through inhibiting DISC complex formation in rat hepatocytes. Biochem Biophys Res Comm 423: 85-90.

74. Fritz JH, Brunner S, Birnstiel ML (2004) The artificial antimicrobial peptide klkllllklk induces predominantly a th2-type immune response to co-injected antigens. Vaccine 22: 3274-3284.

75. Cruciat CM, Dolde C, de Groot RE (2013) Rna helicase ddx3 is a regulatory subunit of casein kinase 1 in wnt-β-catenin signaling. Science 339: 1436-1441.

76. Fullam A, Schröder M (2013) Dexd/h-box rna helicases as mediators of anti-viral innate immunity and essential host factors for viral replication. Biochim Et Biophysica Acta 1829: 854-865.

77. Thompson MR, Kaminski JJ, Kurtjones EA, Fitzgerald KA (2011) Pattern recognition receptors and the innate immune response to viral infection. Viruses 3: 920-940.

78. Oda S, Schröder M, Khan AR (2009) Structural basis for targeting of human rna helicase ddx3 by poxvirus protein k7. Structure 17: 1528-1537.